# Mimics of Yeast tRNA$^{Asp}$ and Their Recognition by Aspartyl-tRNA Synthetase†

Alexey D. Wolfson,‡ Anastasia M. Khvorova,§ Claude Sauter, Catherine Florentz, and Richard Giegé*

*UPR "Structure des Macromolécules Biologiques et Mécanismes de Reconnaissance", Institut de Biologie Moléculaire et Cellulaire du CNRS, 15 rue René Descartes, F-67084 Strasbourg Cedex, France*

*Received April 9, 1999; Revised Manuscript Received July 6, 1999*

ABSTRACT: Assuming that the L-shaped three-dimensional structure of tRNA is an architectural framework allowing the proper presentation of identity nucleotides to aminoacyl-tRNA synthetases implies that altered and/or simplified RNA architectures can fulfill this role and be functional substrates of these enzymes, provided they contain correctly located identity elements. In this work, this paradigm was submitted to new experimental verification. Yeast aspartyl-tRNA synthetase was the model synthetase, and the extent to which the canonical structural framework of cognate tRNA$^{Asp}$ can be altered without losing its ability to be aminoacylated was investigated. Three novel architectures recognized by the synthetase were found. The first resembles that of metazoan mitochondrial tRNA$^{Ser}$ lacking the D-arm. The second lacks both the D- and T-arms, and the 5′-strand of the amino acid acceptor arm. The third structure is a construct in which the acceptor and anticodon helices are joined by two connectors. Aspartylation specificity of these RNAs is verified by the loss of aminoacylation activity upon mutation of the putative identity residues. Kinetic data indicate that the first two architectures are mimics of the whole tRNA$^{Asp}$ molecule, while the third one behaves as an aspartate minihelix mimic. Results confirm the primordial role of the discriminator nucleotide G73 in aspartylation and demonstrate that neither a helical structure in the acceptor domain nor the presence of a D- or T-arm is mandatory for specific aspartylation, but that activity relies on the presence of the cognate aspartate GUC sequence in the anticodon loop.

Transfer RNAs evolved together with the protein synthesis machinery and were subjected to stringent pressures that led to their contemporary L-shaped tertiary structure. This structure fulfills the diverse requirements needed for the versatile tRNA[1] functions in translation. To achieve the L-shaped architecture, nature selected a solution based on a cloverleaf folding, which associates perpendicularly two helical RNA domains joined by two connectors inserted between residues 7 and 10, and 43 and 49 (Figure 1a) (*1*). These helical domains with their distal extremities, the amino acid accepting $CCA_{OH}$ end and the anticodon loop, contain most of the molecular signals that define the biological functions of tRNAs. This is in particular the case for the identity signals, perceived by the aminoacyl-tRNA synthetases (aaRSs), that are responsible for the correct amino acid charging of tRNAs (reviewed in ref *2*). Because of the segregation of the identity signals at the two extremities of tRNA, it is easy to conceive mimics that would associate the distal functional domains by connectors of noncanonical structure (*3*). Such mimics have actually been found in nature. The best known examples are the tRNA-like structures at the 3′-extremities of the genomic RNAs of some plant viruses (reviewed in ref *4*); others, discovered more recently, are the tmRNAs that combine both tRNA and mRNA activities (*5*, *6*). In both cases, the junction between the functional domains is intricate. These natural mimics coexist with canonical tRNAs because they have specialized roles and thus do not interfere with the current functioning of tRNA in translation. Non-natural tRNA mimics recognized by synthetases have been created by rational engineering (reviewed in ref *7*). The first ones were minihelices recapitulating the amino acid accepting branch of those tRNAs with the major identity elements in this domain (*8*). Minihelices corresponding to tRNAs with major identity elements in the anticodon loop, such as tRNA$^{Val}$ and tRNA$^{Asp}$ (*9*, *10*), were also designed. All these minimalist tRNAs were shown to be recognized by synthetases, and some by elongation factors (*11*) and other RNA-recognizing macromolecules (reviewed in ref *3*). Other minimalist tRNAs recognized by synthetases are oligonucleotide duplexes reconstructing an acceptor stem (*12*). A third family of mimics includes anticodon hairpin loops (*13*). More complex RNA structures, with linkers between functional domains, are also conceivable but have been much less studied. The rationale of their design is based on the paradigm that different RNA scaffoldings carrying functional signals at similar locations in space may

† This investigation was supported by Centre National de la Recherche Scientifique (CNRS), Ministère de l'Education Nationale, de la Recherche et de la Technologie (MENRT), Université Louis Pasteur (Strasbourg), and by a grant from the European Community to R.G. (BIO4-CT98-0189). A.D.W. and A.M.K. were supported by short-term fellowships from FEBS, Ministère de la Recherche et de la Technologie, and the French-Russian Fund for Basic Investigation, and C.S. was supported by a fellowship from ARC.

* To whom correspondence should be addressed.

‡ Permanent address: Department of Biochemistry, University of Colorado, Boulder, CO 80309.

§ Permanent address: Department of Molecular, Cellular, and Developmental Biology, University of Colorado, Boulder, CO 80309.

[1] Abbreviations: aaRS, aminoacyl-tRNA synthetase with aa representing Asp, Lys, Met, and Phe, thus for aspartyl-, lysyl-, methionyl-, and phenylalanyl-tRNA synthetase; tRNA, transfer ribonucleic acid.

10.1021/bi9908383 CCC: $18.00 © xxxx American Chemical Society
Published on Web 00/00/0000 PAGE EST: 6.7

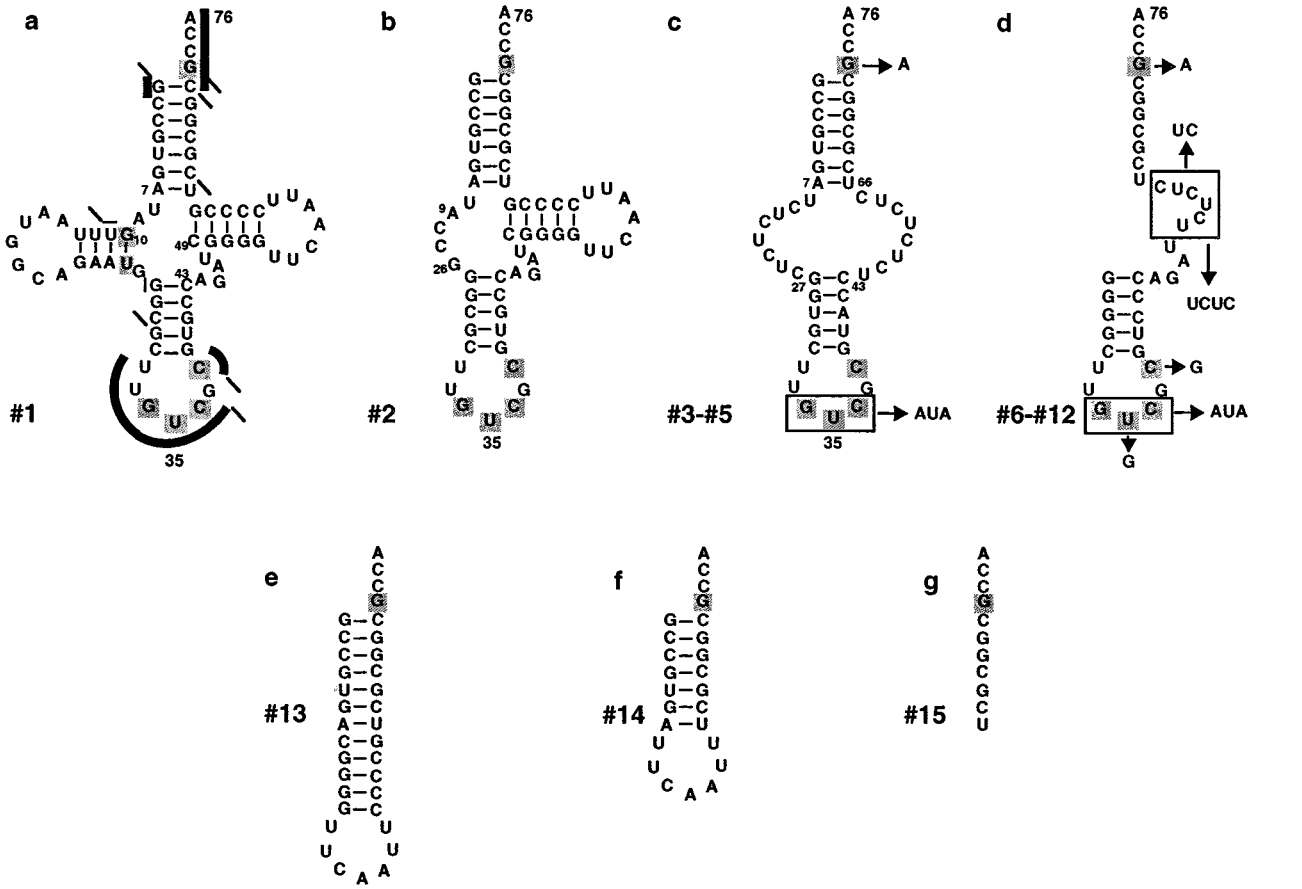


FIGURE 1: Cloverleaf of yeast $tRNA^{Asp}$ (a) and putative folding of its mimics with simplified structure (b−g). The molecules that were investigated are transcripts based on the sequence of native $tRNA^{Asp}$ (*26*) with the first base pair of the amino acid stem changed from U1·A72 to G1·C72. This change facilitates transcription and has no influence on the aspartylation capacity of the transcript (*21*), and this pair is homologous to the native U1·A72 pair for major groove recognition (*27*). Aspartate identity nucleotides are indicated, as well as the mutations introduced in the different constructs. Identification of the molecules is given as in Table 1. The 18 residues that were found in crystallographic contact with AspRS (*28*) are emphasized (with thick lines if contacts involve groups from nucleotide bases or bases and ribose moieties, with thin lines for contacts with riboses only, and by stapled bars for phosphate contacts).

be recognized similarly by proteins specific for these signals. The structure of these mimics may be rather simple if they are intended to be the substrate of a single RNA-recognizing protein and not to have the multifunctionality of canonical tRNAs.

Here we consider mimics recognized by aminoacyl-tRNA synthetases and carrying identity signals from both amino acid-accepting and anticodon ends of tRNA. The simplest version would be a single-stranded oligonucleotide connecting a 3′-$CCA_{OH}$ amino acid acceptor end to a 5′-anticodon. A polyU linked to a 3′-$CCA_{OH}$ end turned out to be a lysine acceptor (*14*), since LysRS requires an UUU anticodon as a major identity element and is only marginally dependent on the nature of the discriminator base N73 (*15*). Aspartate identity, which equally depends on the nature of the discriminator base (G73) and the anticodon (GUC) (*16*), is investigated in the work presented here. Different RNA mimics, based on sequence elements of yeast $tRNA^{Asp}$, have been designed, and their aspartylation by yeast AspRS has been investigated. As predicted, simplified versions of the $tRNA^{Asp}$ molecule were shown to be substrates of AspRS and their activity was shown to be dependent on the presence of the aspartate identity elements. Interestingly, molecules with a single-stranded accepting domain could be aspartylated. Altogether, the displayed experiments outline the subtle interplay between identity elements close to and distant from the catalytic site of AspRS during its functioning; they show also the role of the canonical tRNA architecture for optimizing this functioning. The implications of these findings are discussed.

## MATERIALS AND METHODS

*Materials.* Oligodesoxynucleotides were synthesized on an Applied Biosystems 381A DNA synthesizer using the phosphoramidite method and purified by HPLC on a Nucleosil 120-5-C18 column (Bischoff Chromatography, Zymark-France, Paris, France). L-[$^3$H]Aspartic acid (43 Ci/mmol) was from Amersham France (Les Ulis), and yeast AspRS (*17*) and T7 RNA polymerase (*18*) were purified as described previously. Restriction enzymes *Bst*NI, *Hin*dIII, and *Bam*HI and T4 polynucleotide kinase were from New England Biolabs (Beverly, MA). T4 DNA ligase was from Boehringer Mannheim (Meylan, France).

*Cloning and in Vitro Transcription.* All tRNAs used in this work have been obtained by in vitro transcription of synthetic genes. Each of these genes corresponds to the T7 RNA polymerase promoter region directly connected to the downstream tRNA sequence. The tRNA genes were constructed and cloned according to established methods (*19*, *20*). In vitro transcriptions were performed in reaction mixtures containing 40 mM Tris-HCl (pH 8.1, 37 °C), 22

mM $MgCl_2$, 5 mM dithioerythritol, 0.01% Triton X-100, 1 mM spermidine, nucleoside triphosphates (4 mM each), 5 mM GMP, 0.1 $\mu$g/$\mu$L linearized plasmid, and 15 $\mu$g/mL T7 RNA polymerase. Incubations were carried out for 3 h at 37 °C, and reactions were stopped by phenol/chloroform extraction. Full-length transcripts correctly ending with the $CCA_{OH}$ sequence were purified by preparative electrophoresis on 12% polyacrylamide denaturing gels followed by electroelution (Schleicher & Schuell, Dassel, Germany). The integrity of RNAs in a 10 mM $MgCl_2$ solution was checked by electrophoresis on native gels, and it was found that RNAs migrated as single bands. The concentration of stock solutions of transcripts was determined by absorbance measurements at 260 nm.

*Aminoacylation Reactions.* All aminoacylation reactions (40 $\mu$L) were performed in the assay buffer containing 100 mM Tris-HCl (pH 7.5), 10 mM $MgCl_2$, 3 mM ATP, 30 mM KCl, 50 $\mu$M $^3$H-labeled amino acid, and appropriate amounts of tRNA transcript (within the range of 250−3000 nM for the most of them and 500−8000 nM for minihelices) and synthetase (2−50 nM). Plateau measurements were taken at 1 mM transcript and 400 nM AspRS. Transcripts were renatured before aminoacylation by heating to 65 °C for 90 s and slow cooling to room temperature. AspRS was diluted in bovine serum albumin at a concentration of 5 mg/mL. Incubations were carried out at 25 °C, and 10 $\mu$L samples of aminoacylated tRNA were quenched by spotting on Whatman paper disks (or DE-52 disks for the 11-mer RNA) and counted as described previously (*21*). For variants 9−12 with low aminoacylation plateaus, reactions were performed in the presence of 50 nM AspRS, with an amino acid with a higher specific activity (∼3800 cpm/mL), and in reaction volumes increased to 160 $\mu$L with a corresponding increase in sample volumes to 40 $\mu$L. The kinetic constants were derived from Lineweaver−Burk plots. They represent averages of at least two independent experiments.

*Interpretation of Kinetic Data.* The efficiency of aminoacylation of variants with respect to the wild-type transcripts was appreciated by comparison of the Michaelis−Menten kinetic parameters and in particular by comparison of the specificity constants $k_{cat}/K_M$. Thus, $(k_{cat}/K_M)_{relative} = (k_{cat}/K_M)_{variant}/(k_{cat}/K_M)_{wild-type}$. A more intuitive number, $L$, represents the loss in aminoacylation efficiency of a variant compared to wild-type. It corresponds to the inverse of $(k_{cat}/K_M)_{relative}$ (*22*).

*Structural Modeling of AspRS−RNA Mimic Complexes.* Models of complexes of AspRS and tRNA$^{Asp}$ mimics were constructed on the basis of the crystallographic structure of the yeast AspRS−tRNA$^{Asp}$ complex (*23*). RNA mimics were built with standard stereochemistry using *O* (*24*) and *MANIP* (*25*). They were docked on the synthetase according to the native position of the acceptor stem and anticodon stem loop.

## RESULTS

*Design of tRNA$^{Asp}$ Mimics.* Because of the rules underlying tRNA$^{Asp}$ identity, mimics that would be substrates of AspRS should encompass two domains containing analogues of the G73 discriminator base and the GUC aspartate anticodon. The connector joining these two domains should sterically allow the interaction of the identity elements with the corresponding identity amino acids on the synthetase; it should also provide the necessary binding potential for the synthetase.

The first tRNA$^{Asp}$ mimic, resembling metozoan mitochondrial tRNA$^{Ser}$, lacks the D-arm (Figure 1b). In this molecule, the connection between residues A9 and G26 in tRNA$^{Asp}$ is constituted by a CC stretch so that the 5′-strand of the amino acid accepting stem is joined to the anticodon stem by a five-nucleotide connector. By analogy with conclusions arising from structural probing in solution and modeling of the bovine mitochondrial tRNA$^{Ser(AGY)}$ (*29*), it can be anticipated that this tRNA$^{Asp}$ variant would fold into an L-shaped tertiary structure equivalent to that of canonical tRNA. Structural and functional studies with a similar construct, lacking the D-arm and derived from yeast tRNA$^{Met}$, agree with this view (*30*).

In the construct lacking both the D- and T-arms, the two distal helices are joined by two identical eight-nucleotide $(UC)_4$ connectors (Figure 1c). This type of connection was expected to provide flexibility to the molecule, although a certain rigidity of the construct preventing the correct presentation of the anticodon loop to AspRS cannot be excluded. To provide more structural flexibility and better propensity to adapt on AspRS, a family of other constructs was synthesized (Figure 1d). Here, the amino acid accepting helix is replaced by an 11-mer single strand constituted by the 3′-strand of the helix prolonged by the terminal $GCCA_{OH}$ end of tRNA$^{Asp}$. At its 5′-side, this 11-mer is prolonged by a linker, six to ten nucleotides long, which is attached to the 3′-end of a hairpin loop corresponding to the anticodon arm of tRNA$^{Asp}$. To maintain the best sequence homology with tRNA$^{Asp}$, the sequence of its variable region was maintained in the connector and length variability was brought about by introducing one, two, or three UC dinucleotides at its 3′-side. As control molecules, mini- and microhelices based on the acceptor stem of tRNA$^{Asp}$ (*10*) were reinvestigated as well as an oligonucleotide corresponding to the acceptor end of the tRNA (Figure 1e−g).

The constructs with anticodon loops (Figure 1b−d) contain all the major aspartate determinants. They lack the G10·U25 pair, which is a minor element that acts indirectly via structural effects (*16*). A number of variants were prepared in parallel, with mutations in the identity positions; their choice was dictated by the functional effects, either weak, moderate, or strong, they have in full-length tRNA$^{Asp}$ (*16*, *22*).

*Activity of the tRNA$^{Asp}$ Mimics*. The functional assays of the different mimics derived from the wild-type sequence of tRNA$^{Asp}$, in other words containing the major aspartate identity determinants, are summarized in Table 1. Except for the oligonucleotide (molecule 15) recapitulating the 3′-terminal sequence of tRNA$^{Asp}$ which is completely inactive, all simplified tRNA$^{Asp}$ molecules are functional substrates of AspRS. Activity of the minihelices (13 and 14) is confirmed (*10*), and the constructs without some of the tRNA domains (2, 3, and 6−8) can be charged to plateau levels ranging from 10 to 100%. In terms of catalytic efficiency, the loss of activity measured for the molecule without the D-arm (2) is moderate ($L = 230$). For the mimics with more profound structural alterations (3 and 6−8), the catalytic efficiency is more affected and $L$ values are close to those that are typical for mini- or microhelices ($L \sim 6000$). In contrast, however, with these minimalist tRNAs that bind

Table 1: Kinetic Parameters of the Aspartylation Reactions Catalyzed by Yeast Aspartyl-tRNA Synthetases of $tRNA^{Asp}$ Mimics

| tRNA mimic | nature of the RNA | aminoacylation plateau (%) | $K_M$ (nM) | $k_{cat}$ ($s^{-1}$) | $k_{cat}/K_M$[a] ($\times 10^3\ s^{-1}\ nM^{-1}$) | relative $k_{cat}/K_M$ | $L$ ($x$-fold) |
|---|---|---|---|---|---|---|---|
| canonical $tRNA^{Asp}$ | | | | | | | |
| 1 | wild-type | 98 | 250 | $2.8 \times 10^{-1}$ | $1.1 \times 10^{-3}$ | 1 | 1 |
| $tRNA^{Asp}$ without the D-arm | | | | | | | |
| 2 | wild-type | 100 | 600 | $2.8 \times 10^{-3}$ | $4.7 \times 10^{-6}$ | $4.3 \times 10^{-3}$ | 230 |
| $tRNA^{Asp}$ without the D- and T-arms | | | | | | | |
| 3 | wild-type | 22 | 2050 | $3.7 \times 10^{-4}$ | $1.8 \times 10^{-7}$ | $1.6 \times 10^{-4}$ | 6000 |
| 4 | ac[GUC]$^{Asp}$ → ac[AUA]$^{Tyr}$ | 24 | 1700 | $5.5 \times 10^{-4}$ | $3.2 \times 10^{-7}$ | $2.9 \times 10^{-4}$ | 3400 |
| 5 | G73 → A73 | <1 | nd[b] | nd | nd | nd | nd |
| anticodon/accepting end constructs | | | | | | | |
| 6 | wild-type; $(UC)_{3x}$ | 10 | 490 | $7.8 \times 10^{-5}$ | $1.6 \times 10^{-7}$ | $1.5 \times 10^{-4}$ | 6900 |
| 7 | wild-type; $(UC)_{2x}$ | 11 | 570 | $1.1 \times 10^{-4}$ | $1.9 \times 10^{-7}$ | $1.7 \times 10^{-4}$ | 5800 |
| 8 | wild-type; $(UC)_{1x}$ | 13 | 690 | $1.1 \times 10^{-4}$ | $1.6 \times 10^{-7}$ | $1.5 \times 10^{-4}$ | 6900 |
| 9 | U35 → G35; $(UC)_{3x}$ | 2 | 370 | $8.0 \times 10^{-6}$ | $2.4 \times 10^{-8}$ | $2.2 \times 10^{-5}$ | 46000 |
| 10 | C38 → G38; $(UC)_{3x}$ | 3 | 360 | $9.0 \times 10^{-6}$ | $2.5 \times 10^{-8}$ | $2.3 \times 10^{-5}$ | 44000 |
| 11 | G73 → A73; $(UC)_{3x}$ | <1 | nd | nd | nd | nd | nd |
| 12 | ac[GUC]$^{Asp}$ → ac[AUA]$^{Tyr}$; $(UC)_{3x}$ | <1 | nd | nd | nd | nd | nd |
| minihelices | | | | | | | |
| 13 | wild-type minihelix Asp | 25 | 3200 | $7.7 \times 10^{-4}$ | $2.4 \times 10^{-7}$ | $2.2 \times 10^{-4}$ | 4500 |
| 14 | wild-type microhelix Asp | 17 | 6000 | $9.0 \times 10^{-4}$ | $1.5 \times 10^{-7}$ | $1.4 \times 10^{-4}$ | 7300 |
| oligonucleotide | | | | | | | |
| 15 | 11-mer with $G_{73}CCA_{OH}$ | 0 | nd | nd | nd | nd | nd |

[a] Values varied for replicate experiments by 15%, except for those of variants 9 and 10 (30%). [b] Not determined.

rather poorly to AspRS (*10*), the constructs lacking the D-arm (2) and those with a single-stranded acceptor arm (6−8) bind more tightly, as reflected by $K_M$ values that are like that of canonical $tRNA^{Asp}$ (1). However, the construct without both D- and T-arms (3) behaves kinetically as an aspartate mini- or microhelix (13 and 14). Interestingly, a length variability of the $(UC)_x$ linker in the constructs without the acceptor helix (6−8) has no effect on aspartylation.

*Activity of Variants of $tRNA^{Asp}$ Mimics Mutated at Identity Positions*. Two variants were mutated at the discriminator position (5 and 11). The G73 to A73 mutation decreases aspartylation efficiency by a factor of 160 in the context of both native $tRNA^{Asp}$ (*16*) and the aspartate minihelix (*10*). With these novel variants, this G → A mutation also has dramatic effects on the aminoacylation function, since aspartylation plateaus dropped to less than 1%, and this low activity did not allow for an accurate determination of kinetic parameters.

Two single mutations were introduced in the anticodon loop of the constructs with single-stranded acceptor ends (9 and 10); one concerns the minor identity position C38 (*31*) (10), and the other affects the middle position U35 of the anticodon (*16*) (9). In the context of whole $tRNA^{Asp}$, both U35 → G35 and C38 → U38 mutations lead to ∼20-fold loss in catalytic efficiency (*16*, *31*). In the context of the tRNA mimics, these mutations also have a deleterious effect which is solely due to a decreased $k_{cat}$. Interestingly, however, this effect is less pronounced than in canonical tRNA, since aminoacylation efficiency is only reduced by a factor of ∼6.5 (∼45000/6900) instead of ∼20.

In the two double mutants (4 and 12) derived from the construct lacking the D- and T-arms (3) or that with the single-stranded acceptor end (6), the aspartate anticodon GUC was replaced by a tyrosine anticodon AUA. Such double mutations in the anticodon led to a significant activity decrease in the content of $tRNA^{Asp}$ (*22*). The situation is quite different in the two mutated $tRNA^{Asp}$ mimics (4 and 12). In the molecule lacking both D- and T-arms, the double mutation has no effect on aspartylation efficiency (4); it seems even that the mutant is slightly more active than its wild-type counterpart (3). In contrast, in the molecule with the single-stranded acceptor end (12), the mutation completely abolishes aspartylation activity.

## DISCUSSION

Aside from tRNA-like substrates of aminoacyl-tRNA synthetases based on unconventional foldings, like those with pseudoknotted amino acid acceptor arms (reviewed in ref *4*), only a few atypical structures that are directly derived from the canonical cloverleaf fold are known. The best documented examples are certain animal mitochondrial tRNAs lacking either the D- or T-arm or characterized by helical domains or loops of atypical size and sequence (*32*, *33*). For those molecules, it has been proposed that structural compensations can lead to L-shaped three-dimensional structures where the distance and the mutual orientation of the anticodon and terminal $CCA_{OH}$ are as they are in canonical tRNAs (*34*). Structural investigations of such isolated mitochondrial tRNAs confirmed this view (*35*, *36*) and account for their functionality in the presence of mitochondrial synthetases (*37*−*39*) and other partners of the protein synthesis machinery (*40*, *41*). With regard to tRNAs from the cytoplasm, no atypical structures lacking a domain have been discovered yet in nature. But two such molecules, which can be aminoacylated by yeast cytoplasmic PheRS and MetRS and lack the D-arm, have been produced in vitro. The first one is a 3/4 fragment of $tRNA^{Phe}$ obtained by lead splitting in the D-loop, which acquires aminoacylation capacity only upon removal of the $m^7G$ base at position 46 in the variable region of the fragment (*42*). The second

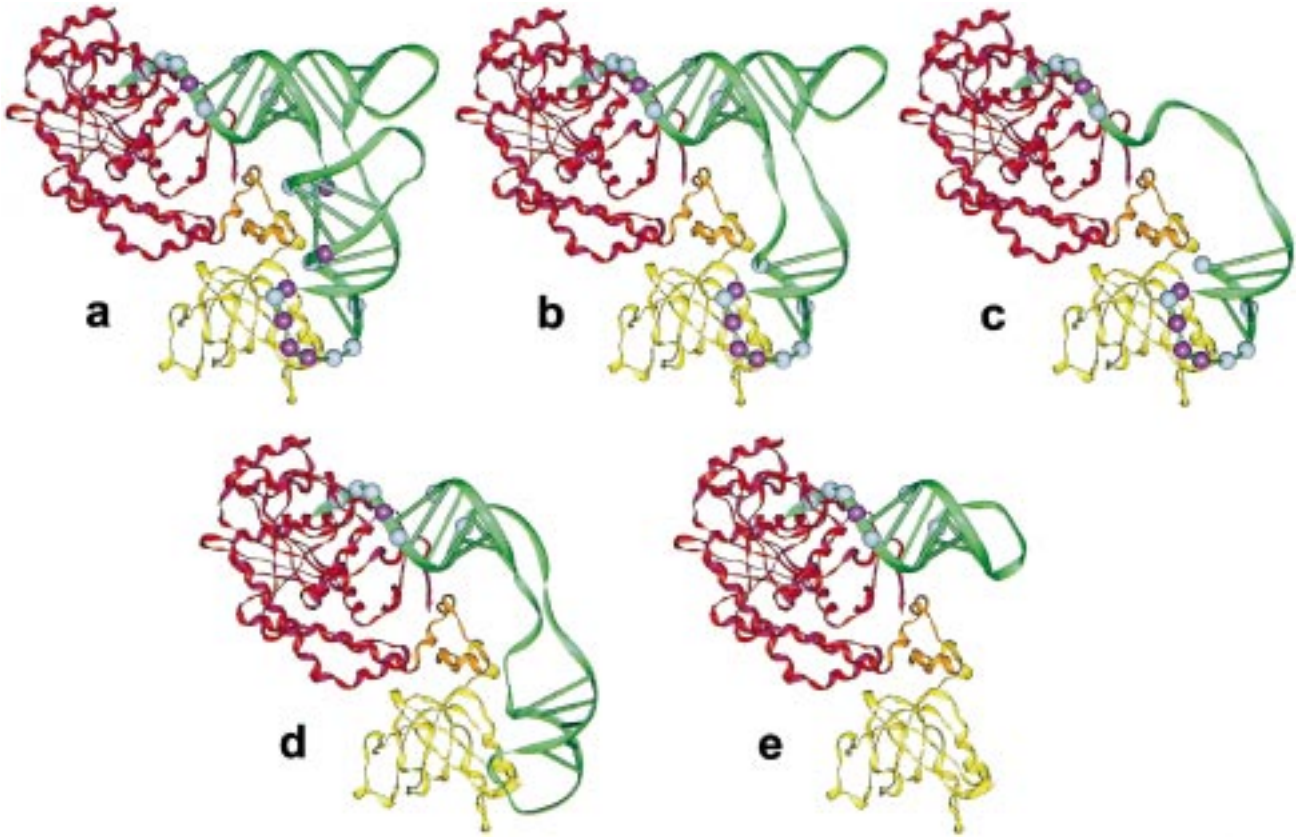


FIGURE 2: Three-dimensional view of the complexes between aspartylatable RNAs and yeast AspRS. (a) Crystallographic structure of the yeast aspartate complex and (b−e) interaction models of the synthetase with tRNA$^{Asp}$ mimics (panels b−e display models with RNAs 2, 6, 3, and 14, respectively). For simplicity, only one subunit of the dimeric aspartate complexes is represented. The modular structure of the AspRS subunit is highlighted with the catalytic domain colored red, the small connecting hinge orange, and the anticodon binding domain yellow. All complexes are displayed in the same orientation. The figure shows the identity elements in the RNAs (as purple spheres) and the nonidentity elements in crystallographic contact with AspRS (as gray spheres) (a), or possibly in contact in the complexes formed with the mimics (b−e). Note that the G10•U25 identity pair is not in direct contact with AspRS (*16*, *28*). In panel d, note that identity elements and contact nucleotides in the anticodon arm of tRNA$^{Asp}$ are not indicated on the model of the mimics whose anticodon arm is displayed in an orientation without direct contact with AspRS. This figure was prepared with *DRAWNA* (*43*).

example is a perfect mimic of mitochondrial tRNA$^{Ser}$, but based on the sequence of yeast initiator tRNA$^{Met}$ (*30*).

In this work, we describe three novel RNA architectures which are recognized by yeast AspRS. The first one (Figure 1b), found in molecule 2, is similar to that of mitochondrial tRNA$^{Ser}$ and of the engineered yeast tRNA$^{Met}$. The RNA with this mimicry retains high aspartylation activity and binds tightly to the synthetase, as reflected by the $K_M$ of aspartylation. The second architecture (Figure 1d), found in molecules 6−8, deviates more from the cloverleaf, since in addition to lacking the D-arm it lacks the T-arm and the 5′-strand of the helix forming the amino acid-accepting arm. In this respect, molecules with such features, in particular single-stranded acceptor ends, partially resemble the 3/4 fragment of tRNA$^{Phe}$ (*42*) and the polyU construct (*14*), which were shown to be substrates of PheRS and LysRS, respectively. Aspartate-accepting RNAs with this peculiar architecture (6−8) interact with AspRS as tightly as the variant without the D-arm (2) and are charged to high plateau levels, although with reduced catalytic efficiency. In both cases, aspartylation is explained by the presence of all the major aspartate identity elements in the mimics, as well as by the structural elements known to make contacts with AspRS as determined by crystallography (*28*). Conformational flexibility of the engineered mimics, especially in the central part of their structure, will allow adaptation of the identity nucleotides at the distal ends of the RNA with their amino acid counterparts on AspRS. This likely possibility is illustrated in Figure 2a−c, which shows models of an AspRS subunit in interaction with the RNA mimics. In variant 2, the core region of the tRNA is essentially maintained, hence recreating the proper L-shaped conformation and allowing a good structural complementarity with AspRS (Figure 2b). In variants 6−8, this core domain no longer exists but is replaced by a flexible connector so that mutual adaptation of RNA and protein becomes possible (Figure 2c). The third architecture, found in variant 3, also lacks both D- and T-arms. But here adaptation with AspRS is more difficult, because the two functional domains of the RNA mimic are linked by two connectors that rigidify its structure (Figure 2d). Thus, association of this molecule on AspRS is weakened (10-fold increase in $K_M$), and proper binding of the anticodon loop with the anticodon domain of AspRS is no longer possible. In other words, the tRNA$^{Asp}$ mimic without the D- and T-arms behaves like a minihelix interacting with AspRS (Figure 2e), a conclusion that correlates well with the similar kinetic behavior of these two types of RNAs (see Table 1).

If true, the above conclusions have implications that can be readily tested. For all aspartylatable RNAs, mutation of the discriminator residue G73 should decrease aminoacylation activity. With regard to the mutations at identity

positions in the anticodon loop, they should have deleterious effects only in those mimics interacting with the anticodon domain of AspRS and be without effect in the minihelix mimics (Figure 2), as was demonstrated with $tRNA^{Asp}$ variants without altered architecture (*16*, *22*). These predictions were verified. Indeed, the G73 → A73 mutation affects dramatically aspartylation in all constructs, and anticodon mutations have effects in the molecules with flexible connectors, thus being able to interact tightly with AspRS (8, 10, and 12). Noticeably, the U35 → G35 ($[GUC]^{Asp}$ → anticodon $[GGC]^{Ala}$) and C38 → U38 variants are only moderately affected in contrast to the double anticodon $[GUC]^{Asp}$ → anticodon $[AUA]^{Tyr}$ mutation which is without effect in variant 4 and leads to a quasi-inactive molecule in variant 12. Likely, the lost binding with the anticodon domain in this molecule does not leave enough interaction potential in this variant to provide efficient functional adaptation of its distal $G73CCA_{OH}$ end in the catalytic site of AspRS and explains its very low activity. In conclusion, the engineered RNA molecules investigated here are specific substitutes of $tRNA^{Asp}$ for aminoacylation, provided they have enough flexibility; otherwise they are minics of the aspartate minihelix, as is variant 3. This flexibility can be achieved by a connector sequence of only six nucleotides between the 11-nucleotide amino acid acceptor oligonucleotide and the anticodon arm. Modeling studies indicate that this length may be reduced to four or even three residues.

With the above conclusions about tRNA conformational flexibility in mind, it is worth revisiting the early observations about the activity of the 3/4 $tRNA^{Phe}$ fragment (*42*) which can be explained by the same rationale. In this fragment, all major phenylalanine identity elements are present, namely, discriminator residue A73, G20, and anticodon triplet GAA (*44*). While this fragment had good affinity for PheRS but no activity by itself, it acquired phenylalanylation capacity upon removal of the $m^7G46$ base (*42*). Although the affinity for PheRS is decreased by a factor of 10, aminoacylation of the fragment is efficient, having a maximal velocity only 10-fold slower than that of native $tRNA^{Phe}$. Likely, this is because removal of the positively charged $m^7G46$ base destabilizes the core region of the tRNA with the consequence that the ionic interactions of G46 with the neighboring phosphate groups, including that of A9 (*45*), are no longer possible. This destabilization, with the possible disruption of the triple G46−(G22−C13) interaction, would provide greater structural flexibility to the fragment, which is supported by UV melting data (*42*), and therefore better adaptability to the synthetase.

The interesting and surprising finding in this work is that aminoacylation does not require the 5′-part of the amino acid acceptor branch of $tRNA^{Asp}$ and therefore does not depend on the mandatory presence of a helical structure before the $GCCA_{OH}$ acceptor 3′-end. This agrees with the limited number of interactions between the 5′-quarter of $tRNA^{Asp}$ and AspRS that are restricted to the backbone contacts with phosphates 1 and 12 and with the ribose of U12 (*28*; see also Figure 1a). This conclusion is well illustrated in the structural models displayed in Figure 2 that clearly show that the 5′-strand of the acceptor helix is fully exposed to the solvent. However, comparing these models suggests that the role of the helix, besides rigidifying the structure of free tRNA, provides in addition the proper architectural framework allowing the optimal adaptation of the 3′-strand with the synthetase. This interpretation explains also the functionality of the atypical PheRS substrate (*42*). As in the aspartate case, the crystal structure of PheRS from *Thermus thermophilus* complexed to cognate $tRNA^{Phe}$ did not reveal any contact of the 5′-quarter of the tRNA with the synthetase (*46*). It is likely therefore that the conclusion arising from this study with the aspartate system can be generalized for other aminoacylation systems, especially with class II synthetases, provided no identity elements are present in the helical stem, like in alanine systems (*47*, *48*) where single strands are inactive (*12*).

These observations also lend further support to the view that the discriminator residue plays a major, if not the primordial role, in many tRNA aminoacylation systems (*10*). In addition, they are in line with a view that was proposed long ago on the basis of tRNA mischarging experiments (*49*), according to which one role of the tRNA body is to permit the correct positioning of the accepting adenosine in the catalytic site of the synthetases. Because this positioning is guided by the interactions with the synthetase in which the RNA can participate, it is understandable that in the case of the aspartate system, the 11-mer oligonucleotide (15) is inactive.

Here we have explored on a rational basis a few possibilities of alternative RNA structures that can be recognized by an aminoacyl-tRNA synthetase. The versatility of such structures most probably is manifold, and it is likey that many more RNA mimics can be selected from RNA libraries with the SELEX technology. This was already done for phenylalanine (*50*, *51*)- and leucine-accepting molecules (*52*), and is under investigation in the aspartate system (*53*), in particular to identify molecules with improved catalytic efficiency. Besides being a way to explore the functioning of synthetases, search of RNA mimics may become a strategy for finding novel inhibitors of protein synthesis.

## ACKNOWLEDGMENT

We thank Stephan Vörtler for comments and critical reading of the manuscript, Anne Théobald-Dietrich for preparation of AspRS, and Benoît Masquida for his help and advice in the use of *MANIP*.

## REFERENCES

1. Moras, D. (1991) *Curr. Opin. Struct. Biol. 1*, 410−415.
2. Giegé, R., Sissler, M., and Florentz, C. (1998) *Nucleic Acids Res. 26*, 5017−5035.
3. Giegé, R., Frugier, M., and Rudinger, J. (1998) *Curr. Opin. Struct. Biol. 8*, 286−293.
4. Florentz, C., and Giegé, R. (1995) in *tRNA: Structure, Biosynthesis, and Function* (Söll, D., and RajBhandary, U. L., Eds.) pp 141−163, American Society for Microbiology, Washington, DC.
5. Felden, B., Hanawa, K., Atkins, J. F., Himeno, H., Muto, A., Gesteland, R. F., McCloskey, J. A., and Crain, P. F. (1998) *EMBO J. 17*, 3188−3196.
6. Komine, Y., Kitabatake, M., Yokogawa, T., and Nishikawa, K. (1994) *Proc. Natl. Acad. Sci. U.S.A. 91*, 9223−9277.
7. Martinis, S. A., and Schimmel, P. (1995) in *tRNA: Structure, Biosynthesis, and Function* (Söll, D., and RajBhandary, U. L., Eds.) pp 349−370, American Society for Microbiology, Washington, DC.
8. Francklyn, C., and Schimmel, P. (1989) *Nature 337*, 478−481.

9. Frugier, M., Florentz, C., and Giegé, R. (1992) *Proc. Natl. Acad. Sci. U.S.A. 89*, 3990−3994.
10. Frugier, M., Florentz, C., and Giegé, R. (1994) *EMBO J. 13*, 2218−2226.
11. Rudinger, J., Blechschmidt, B., Ribeiro, S., and Sprinzl, M. (1994) *Biochemistry 33*, 5682−5688.
12. Musier-Forsyth, K., Scaringe, S., Usman, N., and Schimmel, P. (1991) *Proc. Natl. Acad. Sci. U.S.A. 88*, 209−213.
13. Meinnel, T., Mechulam, Y., Blanquet, S., and Fayat, G. (1991) *J. Mol. Biol. 220*, 205−208.
14. Khvorova, A. M., Motorin, Y. A., Wolfson, A. D., and Gladilin, K. L. (1992) *FEBS Lett. 314*, 256−258.
15. Tamura, K., Himeno, H., Asahara, H., Hasegawa, T., and Shimizu, M. (1992) *Nucleic Acids Res. 20*, 2335−2339.
16. Pütz, J., Puglisi, J. D., Florentz, C., and Giegé, R. (1991) *Science 252*, 1696−1699.
17. Lorber, B., Kern, D., Dietrich, A., Gangloff, J., Ebel, J.-P., and Giegé, R. (1983) *Biochem. Biophys. Res. Commun. 117*, 259−267.
18. Wyatt, J. R., Chastain, M., and Puglisi, J. D. (1991) *BioTechniques 11*, 764−769.
19. Perret, V., Garcia, A., Puglisi, J. D., Grosjean, H., Ebel, J.-P., Florentz, C., and Giegé, R. (1990) *Biochimie 72*, 735−744.
20. Sampson, J. R., and Uhlenbeck, O. C. (1988) *Proc. Natl. Acad. Sci. U.S.A. 85*, 1033−1037.
21. Perret, V., Garcia, A., Grosjean, H., Ebel, J.-P., Florentz, C., and Giegé, R. (1990) *Nature 344*, 787−789.
22. Pütz, J., Puglisi, J. D., Florentz, C., and Giegé, R. (1993) *EMBO J. 12*, 2949−2957.
23. Ruff, M., Krishnaswamy, S., Boeglin, M., Poterszman, A., Mitschler, A., Podjarny, A., Rees, B., Thierry, J.-C., and Moras, D. (1991) *Science 252*, 1682−1689.
24. Jones, A. T., Zhou, J. Y., Cowan, S. W., and Kjeldgaard, M. (1991) *Acta Crystallogr. A47*, 110−119.
25. Massire, C., and Westhof, E. (1999) *J. Mol. Graphics* (in press).
26. Gangloff, J., Keith, G., Ebel, J.-P., and Dirheimer, G. (1971) *Nat. New Biol. 230*, 125−127.
27. Seeman, N. C., Rosenberg, J. M., and Rich, A. (1976) *Proc. Natl. Acad. Sci. U.S.A. 73*, 804−808.
28. Cavarelli, J., Rees, B., Ruff, M., Thierry, J.-C., and Moras, D. (1993) *Nature 362*, 181−184.
29. de Bruijn, M. H. L., and Klug, A. (1983) *EMBO J. 2*, 1309−1321.
30. Senger, B., Aphasizhev, R., Walter, P., and Fasiolo, F. (1995) *J. Mol. Biol. 249*, 45−48.
31. Frugier, M., Söll, D., Giegé, R., and Florentz, C. (1994) *Biochemistry 33*, 9912−9921.
32. Watanabe, Y.-i., Tsurui, H., Ueda, T., Furushiwa, R., Takamiya, S., Kita, K., Nishikawa, K., and Watanabe, K. (1994) *J. Biol. Chem. 269*, 22902−22906.
33. Wolstenholme, D. R., Okimoto, R., and Mcfarlane, J. L. (1994) *Nucleic Acids Res. 22*, 4300−4306.
34. Steinberg, S., and Cedergren, R. (1994) *Nat. Struct. Biol. 1*, 507−510.
35. Wakita, K., Watanabe, Y.-i., Yokogawa, T., Kumazawa, Y., Nakamura, S., Ueda, T., Watanabe, K., and Nishikawa, K. (1994) *Nucleic Acids Res. 22*, 347−353.
36. Hayashi, I., Kawai, G., and Watanabe, K. (1998) *J. Mol. Biol. 284*, 57−69.
37. Kumazawa, Y., Himeno, H., Miura, K.-I., and Watanabe, K. (1991) *J. Biochem. 109*, 421−427.
38. Ohtsuki, T., Kawai, G., Watanabe, Y.-i., Kita, K., Nishikawa, K., and Watanabe, K. (1996) *Nucleic Acids Res. 24*, 662−667.
39. Hayashi, I., Kawai, G., and Watanabe, K. (1997) *Nucleic Acids Res. 25*, 3503−3507.
40. Gebhardt-Singh, E., and Sprinzl, M. (1986) *Nucleic Acids Res. 14*, 7175−7188.
41. Bourdeau, V., Steinberg, S. V., Ferbeyre, G., Emond, R., Cermakian, N., and Cedergren, R. (1998) *Proc. Natl. Acad. Sci. U.S.A. 95*, 1375−1380.
42. Renaud, M., Ehrlich, R., Bonnet, J., and Remy, P. (1979) *Eur. J. Biochem. 100*, 157−164.
43. Massire, C., Gaspin, C., and Westhof, E. (1994) *J. Mol. Graphics 12*, 201−206.
44. Sampson, J. R., DiRenzo, A. B., Behlen, L. S., and Uhlenbeck, O. C. (1989) *Science 243*, 1363−1366.
45. Quigley, G. J., Wang, A. H. J., Seeman, N. C., Suddath, F. L., Rich, A., Sussman, J. L., and Kim, S. H. (1975) *Proc. Natl. Acad. Sci. U.S.A. 72*, 4866−4870.
46. Goldgur, Y., Mosyak, L., Reshetnikova, L., Ankilov, V., Lavrik, O., Khoyreva, S., and Safro, M. (1996) *Structure 5*, 59−68.
47. Hou, Y.-M., and Schimmel, P. (1988) *Nature 333*, 140−145.
48. McClain, W. H., and Foss, K. (1988) *Science 240*, 793−796.
49. Ebel, J.-P., Giegé, R., Bonnet, J., Kern, D., Befort, N., Bollack, C., Fasiolo, F., Gangloff, J., and Dirheimer, G. (1973) *Biochimie 55*, 547−557.
50. Tinkle Peterson, E., Blank, J., Sprinzl, M., and Uhlenbeck, O. C. (1993) *EMBO J. 12*, 2959−2967.
51. Tinkle Peterson, E., Pan, T., Coleman, J., and Uhlenbeck, O. C. (1994) *J. Mol. Biol. 242*, 186−192.
52. Asahara, H., Namek, N., and Hasegawa, T. (1998) *J. Mol. Biol. 283*, 605−618.
53. Pütz, J., Wientges, J., Sissler, M., Giegé, R., Florentz, C., and Schwienhorst, A. (1997) *Nucleic Acids Res. 25*, 1862−1863.


BI9908383